Forecasting district-scale energy dynamics through integrating building network and Long short-term memory learning algorithm

Wei Wang [a], Tianzhen Hong [b], Xiaodong Xu [a,*], Jiayu Chen [c,*], Ziang Liu [a]

[a] *School of Architecture, Southeast University, 2 Sipailou, Nanjing, Jiangsu Province, China*

[b] *Building Technology and Urban Systems Division, Lawrence Berkeley National Laboratory, One Cyclotron Road, Berkeley, CA, 94720, USA*

[c] *Department of Architecture and Civil Engineering, City University of Hong Kong, Y6621, AC1, Tat Chee Ave, Kowloon, Hong Kong*

Abstract: With the development of data-driven techniques, building energy prediction on a district level has attracted increasing attention in recent years for revealing energy use patterns and reduction potentials. However, large-group building data acquisition is more difficult as buildings interact with each other at the city level. To reduce data cost and consider the inter-building impact on the data-driven building energy model, this study proposes a deep learning predictive approach to integrate building networks with a long short-term memory model to create building energy model on a district scale. The building network was calculated via correlations between the energy use intensity of buildings; buildings with high correlation were applied in predictive model to reduce the required number of buildings. To validate the proposed model, five typical building groups with energy use from 2015 to 2018 on two institutional campuses were selected to develop and test the proposed model with the TensorFlow tool. Based on error assessments on the predicted building group energy use, the results suggest that for total building energy use intensity prediction, the proposed model can achieve a mean absolute percentage error of 6.66% and a root mean square error of 0.36 kWh/m^2 , compared to 12.05% and 0.63 kWh/m^2 for artificial neural network model and to 11.06% and 0.89 kWh/m^2 for support vector regression model. Therefore, the proposed model integrating building network and

* Corresponding author. Tel.: +86 (25) 8379-5689; Email: xiaodongxu@seu.edu.cn (Xiaodong Xu)

* Corresponding author. Tel.: +(852) 3442-4696; Email: jiaychen@cityu.edu.hk (Jiayu Chen)

long short-term memory approaches shows good accuracy in predicting building energy use on a district scale.

Keywords: District-scale, building energy modeling; data-driven prediction; building network; long short-term memory network

1. INTRODUCTION

Buildings, as main energy end-users in cities, consume more than 40% of primary energy produced every year [1]. To achieve the goal of carbon reduction and sustainability, many cities have increasingly focused on promoting building energy efficiency. The International Energy Agency's Energy in Buildings and Communities (IEA EBC) Programme annexes suggested that analyzing building energy use patterns is the key to reducing energy use and its associated emissions [2]. Many studies suggested that large-scale building energy modeling can disclose the energy use pattern and effectively reduce energy consumption [3]. Among large-scale building models, data-driven predictive techniques are widely applied and are a significant method alongside with the development of data technologies [4]. Those techniques share the key point that using the historical building energy use data at the city level can reveal energy use pattern with energy cluster analysis [5], and predict the future building energy use trend [6]. In those studies, however, one major challenge usually exists in the urban building energy model (UBEM): how to reduce the size of datasets required for modeling, which, in turn reduce computation complexity and data cost at the city level. Many researchers have started to consider the inter-building effect (IBE) since buildings interact with each other at the city level [7]. and then identify the reference buildings [8]. However, as far as the author's current knowledge, the problem remains unsolved in terms of how to incorporate the effects of buildings and the time-series characteristics of the effects and energy pattern in deep learning approaches for UBEM. Therefore, this study developed a data-driven building energy prediction model on the district level through integration of a building network model and a deep learning approach. The buildings in the district were linked with a building network model, which was created based on the correlation between the energy use of

one building and that of buildings collectively. Buildings with a weak network will be filtered, and the TensorFlow tool was employed in this study to integrate the long short-term memory algorithm for the total energy use prediction. To examine the performance of the proposed model, five building groups were selected from Southeast University in Nanjing, China, and an electricity use dataset was collected for year 2015 to 2018.

2. LITERATURE REVIEW AND BACKGROUND

Studies on UBEM can be divided into two branches—simulation engineering and data-driven techniques—to simulate energy use with detailed building information and historical data-driven models. Therefore, the following review includes current studies about techniques applied in UBEM and the data creation studies at the city level.

2.1 Review of simulation studies on UBEM

With the advancement of information technologies, researchers have developed innovative software and web-based applications for multi-building energy assessments on the district or city levels. For instance, City Building Energy Saver (CityBES), a web-enabled simulation and visualization platform, using EnergyPlus as the simulation engine, focuses on energy modeling and analysis for city building stocks [9]. Based on CityBES, researchers can assess the impacts of building geometry and how a building group performs over time [10]. CitySim simulates urban energy use and provides support for urban planners and stakeholders [11]. City Energy Analyst (CEA) is a computational framework for building energy system analysis and optimization in neighborhoods and city districts [12]. IDA ICE engine is also applied for automated urban building energy models within urban districts embedded with visualization in the geographical information system (GIS) [13]. Remmen et al. developed the TEASER, an open-source tool for an urban energy model with an interface for multiple data sources and export of a ready-to-run Modelica simulation [14]. Rhino can create 3D urban building blocks with plug-ins,

such as Ladybug and Honeybee [15,16]. Honeybee supports detailed daylighting and thermodynamic modeling [17,18]. With these tools, researchers can develop various sophisticated analyses to understand the urban energy dynamics [19,20]. Taleb et al. used Rhino and genetic algorithms to generate a building form cluster that adapts to a dry and hot climate [21]. Davila et al. created energy models and generated 52 use archetypes with the Rhinoceros3D software and EnergyPlus [22]. Although these software packages can explicitly model building energy, they consume enormous computational resources and requires absorbent amounts of data inputs.

2.2 Review of data-driven studies for UBEM

Traditional system-level physical models focus on developing an efficient energy model for individual buildings [40,41]. With an increase in the available building energy data, data-driven models have become feasible for multi-building performance analysis. In the early studies, data-driven models were usually applied to individual buildings. For example, Guo et al. used machine learning-based models to predict energy demands for building heating [42]. Wei et al. applied blind system identification and neural networks to predict office building energy use along with occupancy [43]. Fan et al. assessed deep recurrent neural network-based strategies for short-term building energy predictions [44]. Wang et al. used long short-term memory in predicting internal heat gains for office buildings [45]. In addition to building demand side energy use prediction, some researchers have also studied the prediction of renewable energy systems coupled in buildings, such as wind, solar, and so on. Raza et al. proposed an ensemble predictive framework with five prediction for PV integrated buildings and provide accurate seasonal monthly predictions for smart buildings with rooftop PV [46]. Gonzalez-Aparicio and Zucker provided a regressive approach for accurately predicting the wind power generation with a three-year dataset [47].

Recently, data-driven studies have paid more attention to building energy prediction on a larger scale. For example, Heiple and Sailor estimated daily building-level energy uses with annual building simulation results for prototypical

buildings in Houston, Texas, and matched the prototypes' simulation output for existing buildings [48]. Chen et al. developed an automatic urban building energy model generation and simulation tool that considers neighborhood shadings for city-scale building retrofit analysis [49]. Li et al. analyzed 51 high-performance commercial buildings in the U.S., Europe, and Asia through portfolio analysis and case studies [50]. Kontokosta and Tull proposed a data-driven predictive model of city-scale building energy use and compared three machine learning algorithms (ordinary least squares, support vector regression, and random forest) in an analysis of 20,000 buildings [51]. Deng et al. utilized six regression and machine learning algorithms for urban energy prediction and reported 10%-15% error reductions comparing with statistical models [52]. Robinson et al. utilized a small number of building features with machine learning algorithm for energy consumption prediction and validated the algorithm with the New York City Local Law 84 energy consumption dataset [53]. Fonseca and Schlueter proposed a spatiotemporal model for consumption patterns in neighborhoods and city districts [54]. The model can compute the power and temperature requirements for residential, commercial, and industrial sectors with spatial (building location) and temporal (hourly) dimension analysis. Kalogirou et al. utilized the electricity data of 225 buildings and applied back propagation of neural networks to predict the required heating loads [55]. Hawkins et al. applied statistical and an artificial neural network (ANN) method to identify the determinants for energy consumption of UK higher education buildings [56], resulting in a 34% mean absolute percentage error for electricity use prediction and 25% for heating fuel use prediction. Kavgic applied the Monte Carlo method to predict space heating energy of Belgrade's housing stock [57] and analyzed the sensitivity of uncertainty for a city-scale domestic energy model [58].

2.3 Review of data creation techniques for UBEM

Reducing the size of necessary dataset can effectively reduce the modeling complexity and improve the computational efficiency. Therefore, to create building dataset, the inter-impact and -relationship between building groups have been

analyzed first. The concept of the Inter-Building-Effect was introduced to understand the complex inter-impacts within multi-buildings [23]. Han et al. explored inter-shading and inter-reflection for IBE on building energy performance with two realistic urban contexts in Perugia, Italy [24] and embedding phase change materials into the building envelopes [25]. Reduce-order building models were also advocated to ease the difficulty for computational complexity [26]. Felsmann used reduced order models to explore the district heating or cooling systems [27]. Heidarinejad et al. developed a framework for rapid urban-scale reduced-order building energy model creation with various internal, external, and system thermal loads [28].

Another data creation technique for UBEM is to replicate buildings using typical prototypes. The U.S. Department of Energy has developed 16 commercial reference building types across different climate zones covering 80% of the commercial building stock to support the analysis of urban energy use [29]. Ilaria et al. used the building prototypes to assess the energy saving potentials of residential building stocks [30]. Filogamo et al. applied sample typologies to classify residential buildings stocks and proposed representatives for typical building constructions [31]. Mastrucci et al. analyzed six dwellings types with a GIS-based statistical downscaling approach and utilized linear regression to estimate large scale building stocks [32]. Caputo et al. used four archetypes to characterize the energy performance in a neighborhood built environment [33]. Holistic building energy consumption data can be used for defining reference buildings by investigating the closeness of building groups [34]. Deb and Lee [35] determined the critical variables that influencing energy consumption with a cluster analysis on a small sample of 56 office buildings to represent a large building dataset [36]. Tardioli et al. developed a novel framework, that combines classification, clustering, and predictive modeling to identify 67 representative buildings out of a dataset of 13,614 mixed-function buildings in the city of Geneva [37]. The building prototypes and archetypes can extend the knowledge beyond individual buildings for large-scale neighborhoods or cities, then can be used to develop an energy benchmarking tool and select proper policies [38,39].

In summary, district- and city-scale building energy modeling have been conducted with simulation and data-driven techniques based on detailed and large datasets; therefore, such models require simplified and temporal historical inputs for reliability and efficiency. The remaining sections were developed to fill this research gap. The methodology—including the introduction of prediction models, case study, data-processing, and model configuration—is given in Section 3. Section 4 presents the results on energy use patterns, network between buildings, energy use prediction results, and prediction accuracy assessments. In Section 5, discussions of the findings, implications, and the future work beyond the existing results are deliberated. Finally, Section 6 concludes this study.

3. METHODOLOGY

3.1 Building network and energy prediction models

In this study, the network theory was applied to extract the building network (BN) through historical energy use patterns. The BN investigates the structures of a building group and assesses their inter-relationships. The network connection and relationship coefficients were determined based on historical energy use data, and this study used the Pearson correlation coefficient method to calculate the connections between buildings to establish a BN, which infers the closeness of energy use rather than the tendency of the building energy use pattern. Three machine learning algorithms were adopted to predict district-scale building energy use: long short-term memory (LSTM) networks, artificial neural network (ANN), and support vector machine (SVR). In this study, TensorFlow, an open source machine learning package [59,60] developed by Google Inc., was utilized to integrate the LSTM algorithm and compared with ANN and SVR algorithms. The datasets as the input for the three algorithms consist of building networks and a dataset of building energy use represented in electricity use intensity (EUI), which is calculated as the electricity usage divided by the building floor area.

3.1.1 Long short-term memory network

The LSTM network algorithm is composed of an input layer, a hidden layer, an output layer, a context layer, and a forget layer, as shown in Fig. 1. The hidden layer remembers values over arbitrary time intervals and the other layers regulate the flow of information into and out of the hidden layer. LSTM is an artificial recurrent neural network (RNN) architecture [61] used in the field of deep learning. Unlike feedforward neural networks, an LSTM network can use its internal state (memory) to process input sequences. Therefore, LSTM is widely studied in the unsegmented and connected handwriting recognition [62], speech recognition [63,64], and time-series inference [65].

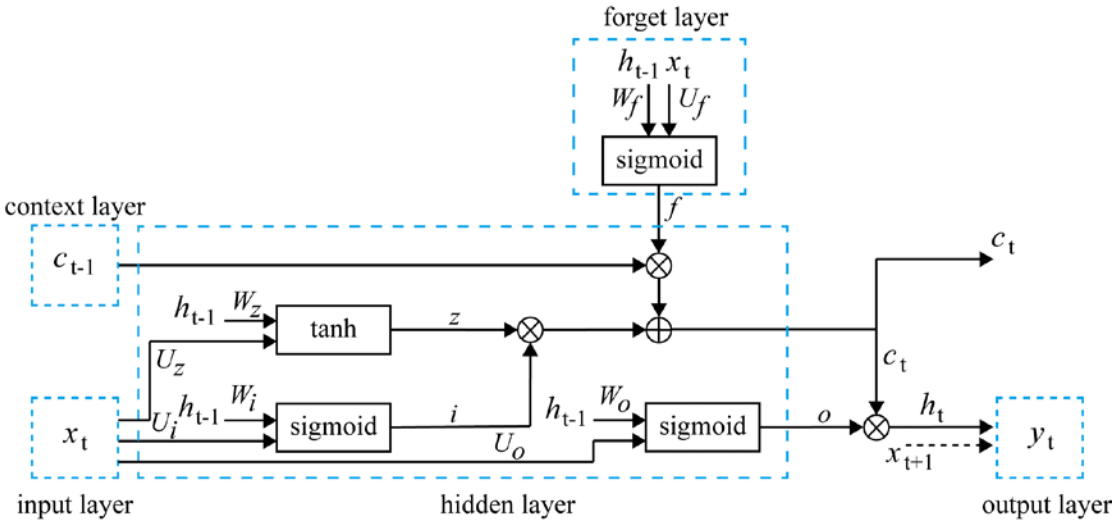

Fig. 1. An illustrative process of the LSTM model with five layers: input layer, hidden layer, context layer, forget layer, and output layer.

In this study, as the building energy use is typical in temporal datasets (time-series data), LSTM is highly suitable for predicting the district-scale building energy use. The input and output layers are assumed to be *X* and *Y*, respectively. *S* is the state layer, and there is also one context layer (C) to store feedback signals for the state layer in the next interval and one forget layer (F) to lead the information, which should be formed based on the current input and previous output:

$$x_t = (EUI_t, BN_t) \rightarrow y_t \quad (1)$$

where $x_t \in X$, $y_t \in Y$. Then, the formulas to represent each layer and connections between layers can be presented as follows:

$$y_t = f(W * x_t + U * h_{t-1} + b) \quad (2)$$

where y donates the output of one layer and includes f_t, i_t, z_t, o_t, and f is the activation function for each layer. W donates the weights of each layer as W_f, W_i, W_z, W_o , and U donates the weights for the last state as U_f, U_i, U_z, U_o. b donates the bias of each layer as b_f, b_i, b_z, b_o. The subscripts (*f, i, z,o*) represent the forget layer, the output and the state of the input layer for next hidden layer, and the output of the hidden layer. The subscript *t* indexes the time step.

The output of the context layer can be a function (Eq. 3) of the forget layer, the context layer at the previous timestep, and the input of the hidden layer. The output of the hidden layer h_t can be updated as Eq. 4.

$$c_t = f_t * c_{t-1} + i_t * z_t \quad (3)$$

$$h_t = o_t * tanhc_t \quad (4)$$

Therefore, the output can be calculated where W_{hy} and b_{hy} are the weight and biases, respectively (Eq. 5).

$$y_t = f(W_{hy}h_t + b_{hy}) \quad (5)$$

3.1.2 Artificial neural network algorithm

The ANN algorithm in this study serves as an optional predictive model for comparison. The ANN algorithm constructs a neural network, which composes simple neuron elements and connection weights, to solve non-linear problems. It can be used for various engineering problems, such as classification, prediction, and pattern recognition. Backpropagation is the most widely used error minimizing system that implement gradient descent to optimize neuron weights to achieve high accuracy. The ANN model has similar arrangement as LSTM but without the context and forget

layers. The results are usually interpreted by an activation function (y_t) (Eq. 6).

$$y_t = f(Wx_t + b) \tag{6}$$

3.1.3 Support vector regression

The SVR algorithm is another alternative algorithm for comparison. SVR integrates hinge loss functions to minimize the prediction error and intends to create a rigid or flexible boundary to include as many samples for reliability as possible. The errors of SVR can be determined by following equations.

$$Min \frac{1}{2} \|\omega\|^2 \tag{7}$$

$$subject\ to \begin{cases} y_t - \langle \omega, x_t \rangle - b \leq \varepsilon \\ \langle \omega, x_t \rangle + b - y_t \leq \varepsilon \end{cases} \tag{8}$$

where x_t is training samples and y_t is the label. ε is an arbitrarily determined boundary. $\langle \omega, x_t \rangle$ is the inner product and b is a bias. Samples within the hinge boundary satisfy the conditions in Eq. 8.

3.2 Case Study

3.2.1 Data description

The validation experiment was conducted on the campus of Southeast University (SEU) in Nanjing, China. The university has two main campuses; the old campus has a gross area of 0.6 km^2 with 53 buildings while the new campus has a gross area of 2.5 km^2. Fig. 4 shows the layout of both campuses.

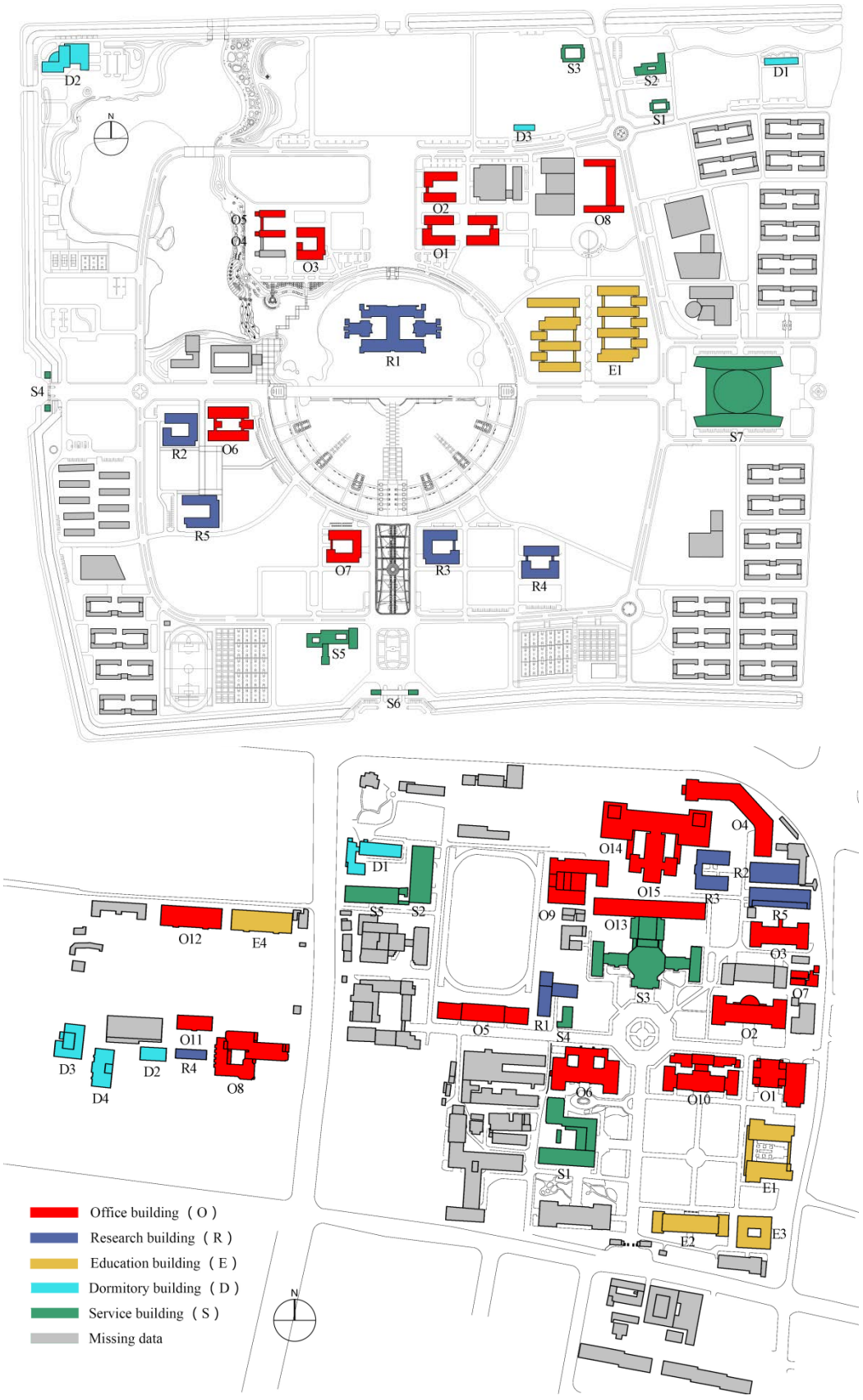

Fig. 4. Layout of case buildings on the new campus (top) and the old campus(below) with different building groups.

This study applied the analysis based on the actual building energy use (electricity) combined with building floor areas. The datasets are provided by the SEU Department of General Affairs (DGA). As shown in Fig. 4, five major building types are identified: office buildings (O), research buildings (R), education buildings (E), dormitory buildings (D), and service buildings (S). Meanwhile, the functions of those buildings (O, R, E, D, S) are easily visible by their names, and services buildings denote the retail stores, canteen, security, equipment rooms, and so on. The buildings' monthly electricity use datasets were collected from January 2015 to October 2018. After a preliminary analysis, several observations were identified: (a) electricity use of some buildings is missing for a long period (more than 3 months); (b) some buildings have 1-2 months of missing electricity data; and (c) DGA faculties merged the electricity use for multiple months. Those buildings have the problematic data are marked in grey. Finally, after eliminating buildings with data quality issues, 33 buildings were selected from the old campus (15 office buildings, 5 research buildings, 4 education buildings, 4 dormitory buildings, and 5 service buildings) and 23 buildings were selected from the new campus (8 office buildings, 4 research buildings, 1 education building, 3 dormitory buildings, and 7 service buildings).

3.2.2 Data preprocessing

This study assumed there are no significant functional changes of the experimental buildings during the experiment period. The inputs are formulated as follows

$$x_{k-1}^{p}: x_{k}^{p}: x_{k+1}^{p} = x_{k-1}^{c}: x_{k}^{c}: x_{k+1}^{c} \tag{9}$$

and

$$x_{k-1}^{c} + x_{k}^{c} + x_{k+1}^{c} = x_{total}^{c} \tag{10}$$

where x_k is the electricity data at time step k. p and c denote the previous year and current year, respectively. x_{total} is the total electricity use of time step $k-1$, k, $k+1$. Then,

$$x_k^c = \frac{x_k^p * x_{total}^c}{x_{k-1}^p * x_k^p + x_k^p + x_k^p * x_{k+1}^p} \quad (11)$$

While pre-processing the raw data, the exponential moving average (EMA) filter is applied to smooth electricity use profiles for its computational efficiency and causality (Eq. 12).

$$\bar{x}_k = \frac{n}{n+1}\bar{x}_{k-1} + (1 - \frac{n}{n+1})x_k \quad (12)$$

Where $\bar{x}_k$ and $\bar{x}_{k-1}$ are the EMA filtered value at time step k and k-1, respectively. Once the measured electricity data has been filtered, those data can proceed as the input data for the three machine learning techniques.

3.3 Model integration and error assessment

Fig. 2 shows the LSTM graph used in this study in TensorBoard, which is the visualization tool of TensorFlow to help understand the processing of model training and learning in the neural networks. The LSTM cell is the structure shown in Fig. 1. Compared with LSTM, the ANN algorithm has a simplified neural structure, which includes the input, hidden, and output layers. While for weights learning, the gradient descent rule (Adagrad method) was selected for the learning process. The gradient descent rule is the basic method to minimize the loss function in machine learning discipline, the details of which are therefore not included in this study. For ANN and LSTM initialization, weights and biases are randomly selected while in the training iteration. Then weights and biases can be updated based on loss function (L) as

$$L = \frac{\sum_{t=1}^{n}(y_t - y_{a,t})^2}{n} \quad (13)$$

where n is the size of training time samples, and $y_{a,t}$ is the actual electricity use. For activation function selection, the $f_{sigmoid}$, described as Eq. 6, is used for the output of the input, forget, and hidden layers. The f_{tanh}, described as Eq. 7, is used for the state function of the input layer, and f_{ReLU} is used for the final output function. The equations are given below.

$$f_{sigmoid}(\mathrm{x}) = \frac{1}{1+e^{-x}} \tag{14}$$

$$f_{tanh}(\mathrm{x}) = \frac{1-e^{-2x}}{1+e^{-2x}} \tag{15}$$

$$f_{ReLU}(\mathrm{x}) = \max(x, 0) \tag{16}$$

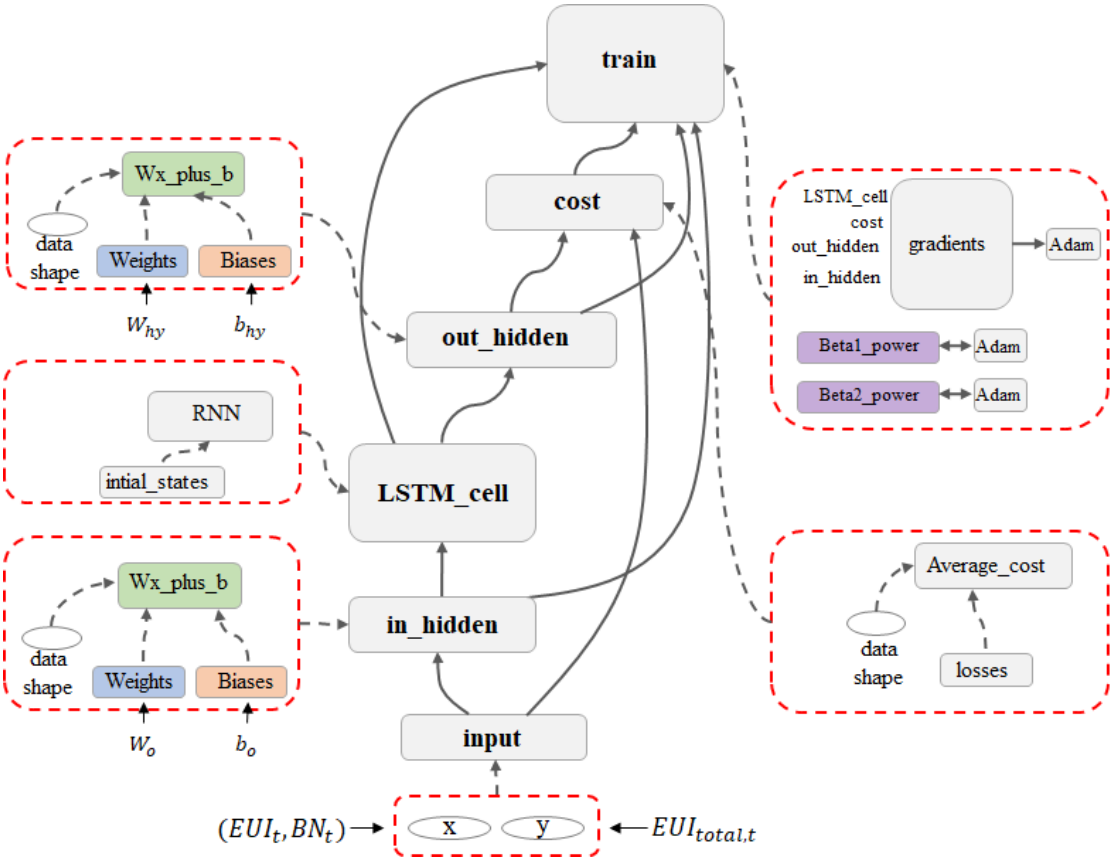

Fig. 2. The LSTM processing and structure visualized in TensorBoard.

As buildings have different capacities and then different EUI values, to simplify the model, this study normalized the inputs of EUI values based on their size (i.e., total floor area). For the BN selection, only the buildings with an absolute correlation higher than 0.6 were selected in the building network, where the correlation denotes the building network by calculating correlation between the EUI of one building and the total EUI of all buildings. For model cross validation, this study selected the cross-fold validation method, which splits the time-series dataset from year 2015 to year 2017 into 80% for the training and 20% for the validation, and total EUI of all buildings in the corresponding group in year 2018 (10 months) as prediction for the

test. The entire prediction process is illustrated in Fig. 3. For ANN and LSTM, the maximum training iterations are 100000, the size of the hidden layer is 10, the learning rate is 0.1, the batch size is 3, and the activation function is RELU. For SVR, this study applied the grid search method to match best set of parameters for model configuration, where kernel function is among rbf, sigmoid, and poly. In the model, C equals 1, 10, 100, and 1000, and gamma equals 0.1, 0.2, 0.3, 0.4, and 0.5, respectively. This study used Python 3.6 with TensorFlow 1.12 for data preprocessing, model training, and prediction.

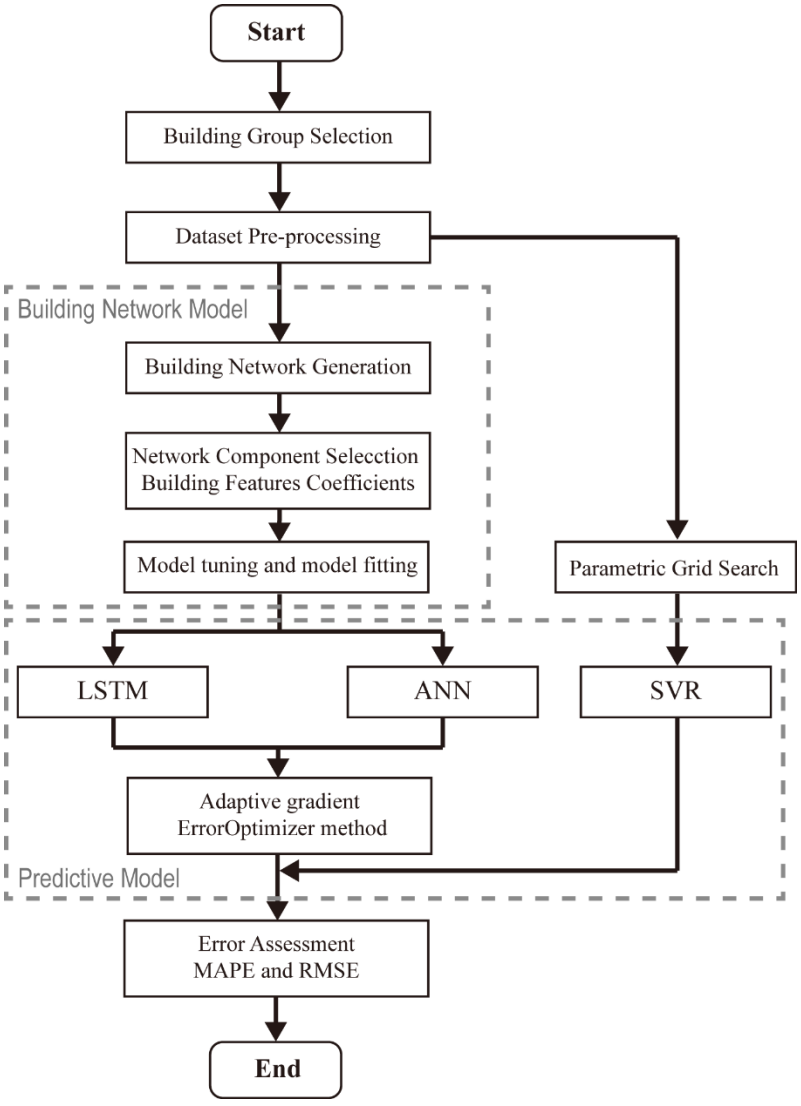

Fig. 3. Scheme of the proposed predictive model and the comparison process in this study.

To assess the model performance, two indices were used to compare the results

for accuracy:

Mean absolute percentage error (MAPE): the mean percentage error between the predicted EUI (y_t) and the actual EUI of the building $(y_{a,t})$, where n is the sample size:

$$MAPE = \frac{1}{n}\sum_{i=1}^{n}\left|(y_t - y_{a,t})/y_{a,t}\right| \quad (17)$$

Root mean squared error (RMSE): the magnitude of the estimation error:

$$RMSE = \sqrt{\frac{\sum_{t=1}^{n}(y_t - y_{a,t})^2}{n}} \quad (18)$$

4. RESULTS

4.1 Building EUI

Figs. 5 and 6 show the building EUI distributions on the old campus and the new campus. For brevity, the presented EUI result is the average of building electricity use from year 2015 to 2017. Fig. 7 shows the building network between buildings on the old and new campuses, respectively.

Fig. 5. The average building EUI results distribution on the SEU new campus.

Fig. 6. The average building EUI results distribution on the SEU old campus.

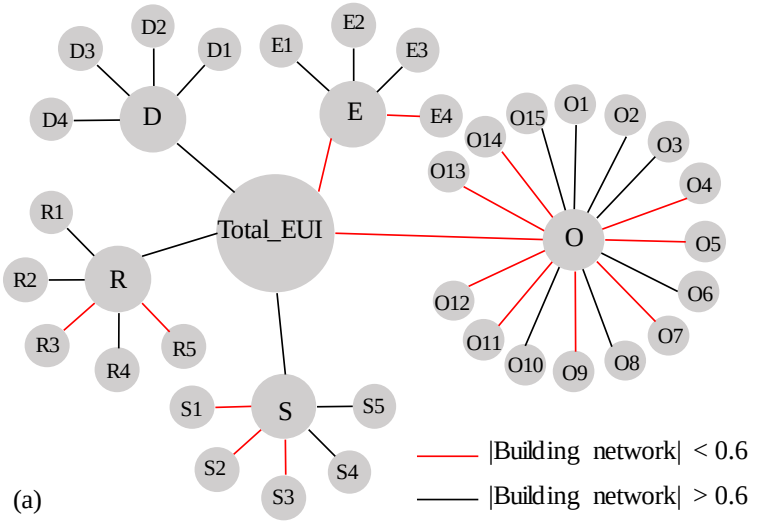

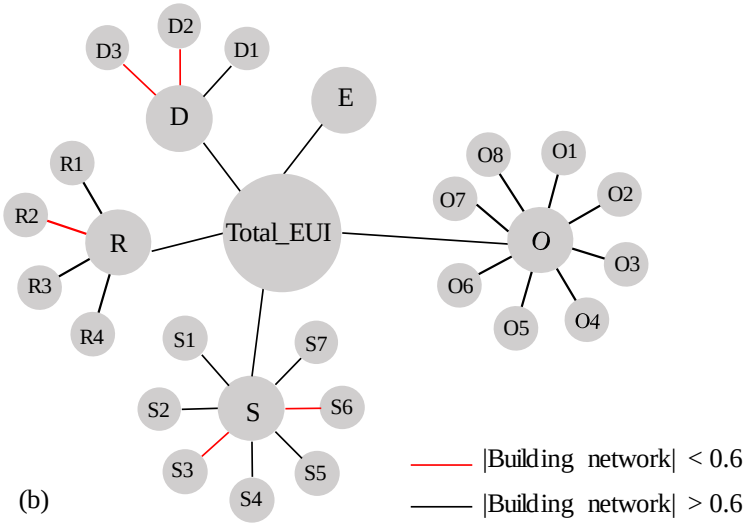

Fig. 7. The example illustration of the building network in (a) the old campus and (b) the new campus.

Tables 1-5 show the total minimum, maximum and standard deviation of EUI results for each type of building in years 2015, 2016, and 2017, respectively. On the old campus, the total EUI of the office buildings significantly increased from 58.62 kWh/m^2 to 89.89 kWh/m^2 by year, and the standard deviation of EUI between office building groups also increased considerably, which shows energy use is not steady. Compared with the old campus, the EUI of office buildings on the new campus did not show one clear trend; however the standard deviation is much higher than of the old campus and the variation between individuals is much bigger. Research buildings on both two campuses consumed more energy in year 2017 when compared with energy in year 2015 although the differences are not very distinct. Similarly, the standard deviation for the new campus is much higher than for the old campus.

Table 1. The total, minimum, maximum and standard deviation of EUI results (kWh/m^2) for office buildings in years 2015, 2016, and 2017.

	Old campus			New campus		
	2015	2016	2017	2015	2016	2017
Total EUI	58.62	68.98	89.89	41.24	39.24	48.53
Min.	21.12	23.06	18.32	3.48	2.81	4.06
Max.	125.08	134.36	225.70	196.69	219.55	315.65
Std.	33.97	35.37	56.04	60.13	64.37	93.28
Note: total areas of old and new campuses are 114088 and 153722 m^2, respectively.						

Table 2. The total, minimum, maximum and standard deviation of EUI results (kWh/m^2) for research buildings in year 2015, 2016, and 2017.

	Old campus			New campus		
	2015	2016	2017	2015	2016	2017
Total EUI	31.03	26.08	40.98	54.62	56.58	60.54
Min.	11.24	4.46	3.57	4.66	12.81	10.59
Max.	66.70	66.46	83.86	135.76	145.02	171.78
Std.	21.66	25.47	31.14	51.01	52.70	64.14
Note: total areas of old and new campuses are 9416 and 101206 m^2, respectively.						

Table 3. The total, minimum, maximum and standard deviation of EUI results (kWh/m^2) for education buildings in year 2015, 2016, and 2017.

	Old campus			New campus		
	2015	2016	2017	2015	2016	2017
Total EUI	41.09	49.61	50.43	23.92	30.3	27.28
Min.	20.22	18.23	18.37	-	-	-
Max.	83.59	97.50	101.16	-	-	-
Std.	26.17	30.46	32.57	-	-	-
Note: total areas of old and new campuses are 19566 and 67219 m^2, respectively.						

Table 4. The total, minimum, maximum and standard deviation of EUI results (kWh/m^2) for dormitory buildings in year 2015, 2016, and 2017.

	Old campus			New campus		
	2015	2016	2017	2015	2016	2017
Total EUI	20.39	35.74	67.58	52.48	38.04	58.88
Min.	14.00	32.58	32.27	28.41	36.32	26.91
Max.	55.58	51.69	99.40	64.93	39.96	73.09
Std.	17.51	7.72	25.01	15.01	1.26	19.07
Note: total areas of old and new campuses are 26285 and 24656 m^2, respectively.						

Table 5. The total, minimum, maximum and standard deviation of EUI results (kWh/m^2) for service buildings in year 2015, 2016, and 2017.

	Old campus			New campus		
	2015	2016	2017	2015	2016	2017
Total EUI	73.45	77.71	80.94	36.35	18.45	15.56
Min.	4.02	3.64	3.68	25.08	2.02	1.53
Max.	612.69	595.87	618.36	211.84	293.03	59.62
Std.	236.73	228.05	237.04	64.84	94.19	19.13
Note: total areas of old and new campuses are 22654 and 45094 m^2, respectively.						

Since there is only one education building with an available electricity dataset for the new campus, the minimum, maximum, and standard deviation results of EUI of this building are ignored in Table 3. Comparing the total EUI results, both campuses have a relatively steady trend of energy use across three years, although the old campus consumed more energy than the new campus. Dormitory buildings have the lower standard deviations compared with other types of buildings. For example, the standard deviation in new campus is only 1.26 in year 2016. The EUI results of the two campuses show that energy usages also increased compared to years 2015 and 2017. In addition, the energy use increased for services buildings on the old campus, but decreased on the new campus. However, the reasons for the different EUI results

between two campuses might be difficult to pinpoint. Although the function of each type of building group is the same, the occupancy rate, end-user behavior, and operation varied significantly, highlighting that further exploration is needed.

The building networks consist of two parts, (a) between the EUI of each individual building and the total EUI of the corresponding type of buildings; (b) between the total EUI of different types of building groups and the total EUI of the corresponding campus. The building network is applied to filter those buildings, which have a weak network to the total EUI. The network at the current timestep is dynamically created using the previous three-month electricity use data; Fig. 7 presents building networks for January 2017. For those buildings indicating weak networks, the prediction algorithm excluded them from the algorithms. For example, on the old campus, for the building group D, all three buildings (D1, D2, D3) are inputs for models; however, for the building group E, building E1, E2, and E3 are inputs, but E4 is not.

4.2 Prediction model accuracy

Figs. 8-13 show the model prediction results of the district-level building electricity use for different building types. From those figures, it can be seen that, although the buildings have the same functions, the EUIs are quite different between the old and new campus. Usually, buildings on the old campus have higher EUIs than those on the new campus. SEU planned to gradually move all disciplines from the old campus to the new one starting in year 2015. Most buildings on the new campus have low occupancy rates. As discussed in the methodology, the LSTM, ANN, and SVR models are compared to validate the prediction accuracy, using the TensorFlow tool.

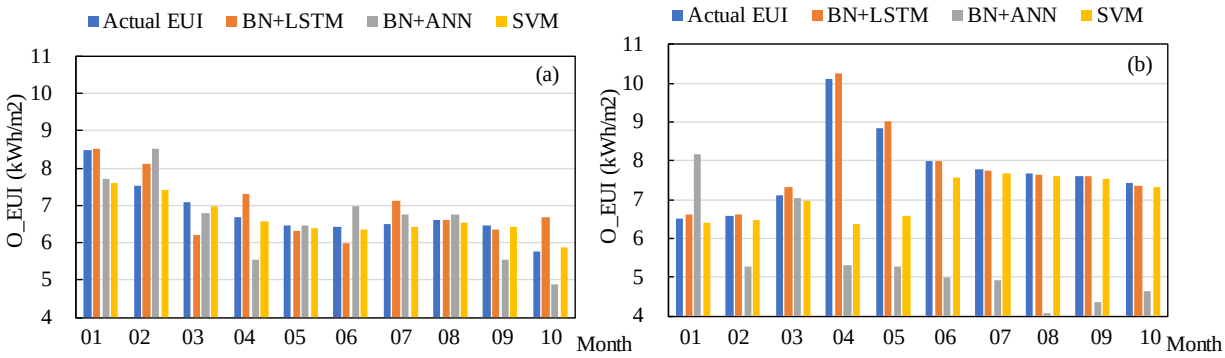

Fig. 8. EUI prediction results for office buildings using LSTM, ANN, and SVR, respectively, for (a) the old campus and (b) the new campus.

Table 6. Prediction accuracies of LSTM, ANN, and SVR models for office buildings.

	Old Campus		New Campus		Total	
	MAPE	RMSE	MAPE	RMSE	MAPE	RMSE
BN+LSTM	6.73%	0.55	1.05%	0.11	3.89%	0.4
BN+ANN	8.82%	0.70	33.6%	2.98	21.21%	2.17
SVR	2.30%	0.30	7.75%	1.40	5.01%	1.01

For office building type (O) in Fig. 8, the actual EUI of office buildings is gradually increasing on the new campus while decreasing on the old campus and in a few years, the office building EUI on the old campus will gradually decrease to a very low level. Table 6 concludes the accuracies of the LSTM, ANN, SVR models for total the EUI prediction for office buildings. The table clearly shows that all three models can provide good prediction accuracies for the old campus with MAPE of 6.73%, 8.82%, and 2.3% for the LSTM, ANN, and SVR models, respectively, and 1.05%, 33.6%, and 7.75%, respectively, for the new campus. According to the total accuracy, LSTM can achieve better prediction results than the ANN algorithm and a little better than the SVR model where MAPE accuracies are 3.89%, 21.21%, and 5.01%, respectively. Additionally, overall results show that the LSTM model has the lowest RMSE (0.4 kWh/m^2) and that prediction results are much steadier. Looking at Fig. 9 for research buildings, interestingly, the trend of total EUI is opposite to the trend of office buildings. Results also show that the total EUI of research buildings is relatively lower than that of office buildings. On the old campus, LSTM model can have good performance as the SVR and ANN models also perform good predictions;

however, on the new campus, the SVR model has the best performance with a MAPE of 4.14% and RMSE of 0.11 kWh/m2, while the ANN model is poor, which shows that the MAPE reaches 53.82% and RMSE reaches 1.47, respectively. Overall, the LSTM and SVR models can achieve over 90% prediction accuracy.

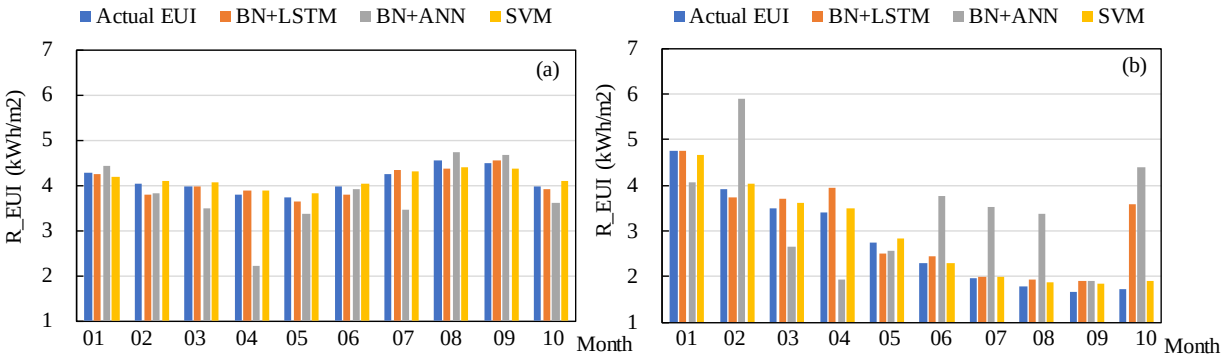

Fig. 9. EUI prediction results of research buildings using the LSTM, ANN, and SVR models, respectively, for (a) the old campus and (b) the new campus.

Table 7. Prediction accuracies of the LSTM, ANN, and SVR models for research buildings.

	Old Campus		New Campus		Total	
	MAPE	RMSE	MAPE	RMSE	MAPE	RMSE
BN+LSTM	2.3%	0.10	17.26%	0.63	9.92%	0.45
BN+ANN	11.07%	0.61	53.82%	1.47	32.45%	1.12
SVR	2.58%	0.13	4.14%	0.11	3.22%	0.1

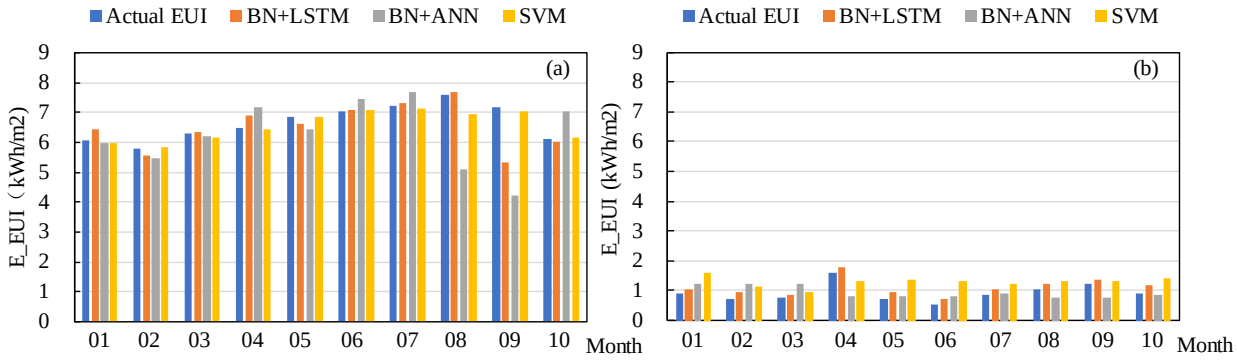

Fig. 10. EUI prediction results of education buildings using the LSTM, ANN, and SVR models, respectively, for (a) the old campus and (b) the new campus.

Table 8. Prediction accuracies of the LSTM, ANN, SVR models for education buildings.

	Old Campus	New Campus	Total

	MAPE	RMSE	MAPE	RMSE	MAPE	RMSE
BN+LSTM	5.14%	0.62	22.13%	0.19	13.63%	0.46
BN+ANN	12.59%	1.29	35.68%	0.40	24.14%	0.96
SVR	1.90%	0.21	56.68%	0.49	29.26%	0.38

Education buildings have very close trends for the old and new campuses, however, the current education buildings on the new campus consume much less electricity than those on the old campus. The results show that for the old campus, those models can all achieve good accuracies, especially the LSTM and SVR models. Conversely, on the new campus, the performance decreases, especially in the SVR model. Therefore, prediction accuracies in total show that the LSTM model has the best performance and the MAPE is about 13.63%. For building type D, the EUI decreases gradually on the old campus, but, on the new campus, increases and then decreases in April. In such a building type, results clearly show that the LSTM model can have the best performance, although the SVR and ANN models can predict EUI well when considering MAPE, which are 2.94%, 9.09%, and 8.48%, respectively. However, the RMSE shows that the LSTM model can reach the lowest of 0.27 kWh/m^2. The same case can be found in service buildings. The LSTM model has obviously better accuracies for EUI predictions for the old, new, and both campuses. Fig. 13 and Table 11 show the prediction results and accuracy assessment for total energy use on the old and new campuses. Both campuses have very close EUI trends, and the EUIs are also approximate, except for the EUI in April when the old campus consumed more electricity. On the old campus, the LSTM and SVR models achieved approximately accurate EUI predictions with MAPEs of 11.66% and 11.39%, respectively, however, comparing the RMSEs of the two models, the LSTM model shows the smallest root square error with only 0.51 kWh/m^2, while the SVR model has an RMSE result of 1.15 kWh/m^2. For the ANN model, the accuracy reaches 82.83%. Overall, all models achieved good performance in predicting the EUI for all buildings, and comparatively LSTM has more accurate predictions. The MAPE results for the three models are 6.66%, 12.05%, and 11.60%, respectively, and the RMSE results are 0.36, 0.63, and 0.89 kWh/m^2, respectively.

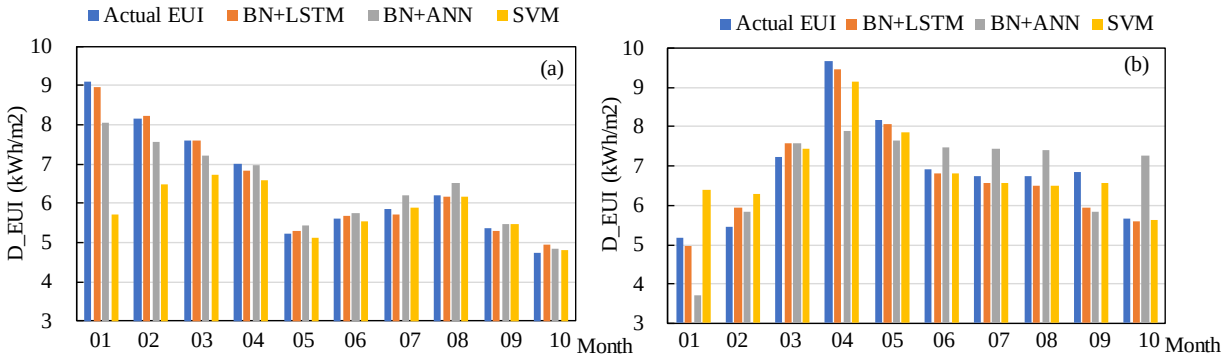

Fig. 11. EUI prediction results of dormitory buildings using LSTM, ANN, and SVR models, respectively, for (a) the old campus and (b) the new campus.

Table 9. Prediction accuracies of the LSTM, ANN, and SVR models for dormitory buildings.

	Old Campus		New Campus		Total	
	MAPE	RMSE	MAPE	RMSE	MAPE	RMSE
BN+LSTM	1.5%	0.11	4.3%	0.37	2.94%	0.27
BN+ANN	4.59%	0.44	13.6%	1.03	9.09%	0.79
SVR	8.37%	1.24	8.59%	0.93	8.48%	1.10

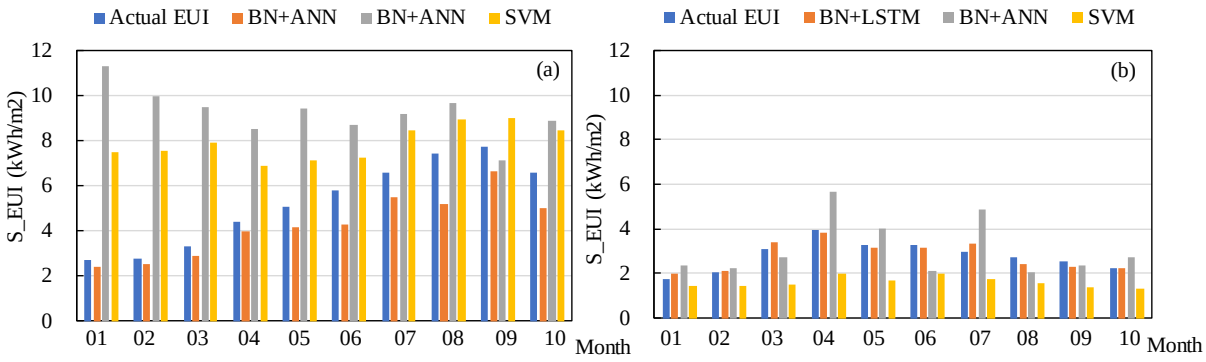

Fig. 12. EUI prediction results of service buildings using the LSTM, ANN, and SVR models, respectively, for (a) the old campus and (b) the new campus.

Table 10. Prediction accuracies of the LSTM, ANN, and SVR models for service buildings.

	Old Campus		New Campus		Total	
	MAPE	RMSE	MAPE	RMSE	MAPE	RMSE
BN+LSTM	17.08%	1.16	6.48%	0.21	11.78%	0.83
BN+ANN	110.71%	4.75	27.13%	0.99	68.92%	3.43
SVR	30.35%	3.00	40.62%	1.27	55.48%	2.3

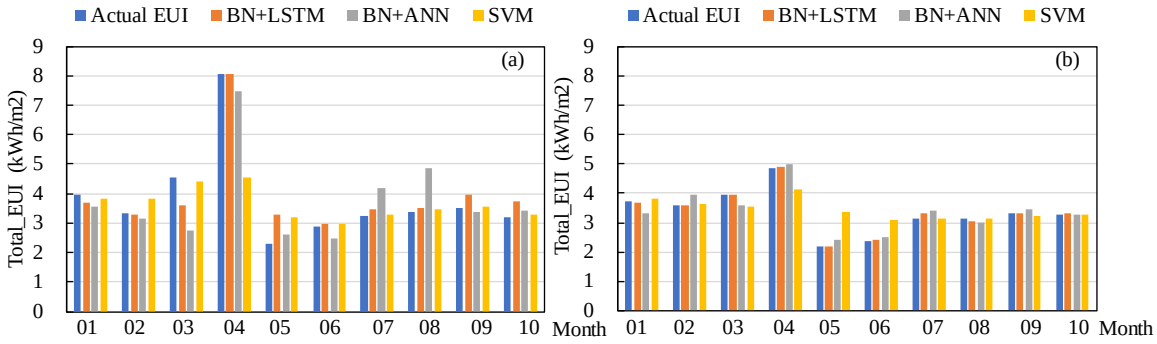

Fig. 13. EUI prediction results of total buildings using the LSTM, ANN, and SVR models, respectively, for (a) the old campus and (b) the new campus.

Table 11. Prediction accuracies of the LSTM, ANN, and SVR models for total buildings.

	Old Campus		New Campus		Total	
	MAPE	RMSE	MAPE	RMSE	MAPE	RMSE
BN+LSTM	11.66%	0.51	1.65%	0.07	6.66%	0.36
BN+ANN	17.17%	0.85	6.94%	0.26	12.05%	0.63
SVR	11.39%	1.15	11.81%	0.51	11.60%	0.89

5. DISCUSSION

To predict multi-building energy use with data-driven models, this study proposed to integrate the building network with the long short-term memory network in the prediction model. Two models, ANN and SVR, were used to compare the performance of models. The total results clearly show that the proposed BN+LSTM model has better accuracies than the ANN and SVR models; they also suggested that, even with a reduced dataset, considering the relationship between buildings and the time-series characteristics can benefit multi-building energy use prediction. On the other hand, dynamic energy use awareness is critical to knowing where and how energy is being consumed. Large-scale buildings' energy prediction can estimate the dynamic energy use, which is one key feature of grid-interactive efficient buildings [66]. Forecasting the demand at building side on the district level is also important objective of this study, to support electricity supply optimization. A campus consists of big groups of buildings in a region and has significant energy-savings potentials. In current campus development, building electricity datasets are usually obtained

manually or inferred from electricity bills. In upcoming sustainable campus projects, smart meters can be applied to monitor the electricity use of every building and upload the data to a server. The TensorFlow tool can provide application program interfaces (APIs) to help visualize the implementation of machine learning techniques. Those APIs can efficiently and conveniently enhance users' ability to create online modeling of large-scale building energy uses with machine learning techniques. Additionally, the LSTM in TensorFlow proposed in this study provides high accuracies for energy use prediction for a sustainable campus and intelligent energy management. With increasing attention focused on building integrated photovoltaics (BiPV), forecasting large-scale building energy uses can provide significantly predictive supports to manage electricity production of BiPV, allocate energy and identify cost-efficient savings opportunities across the city based on building energy loads. In this way, this study can also contribute to studies of the corresponding micro-grids that can be implemented on campuses.

However, this study still yields some limitations and unsolved issues. Firstly, for large- or city-scale building energy prediction, one big challenge is data deficiency, which exists because some buildings in urban block area have no energy records at all, some miss energy data in some months, and so on. However, detailed building datasets are usually difficult to acquire, and a limited dataset can restrain accuracies of machine learning techniques so that reasonable dataset preprocessing might influence the validation of algorithms. On one hand, while dealing with this problem, this study assumed the energy use pattern (trend) is similar in each year. For brevity, however, this study did not discuss the impact of different preprocessing method in the machine learning models, which would provide one vital research for modeling city-scale building energy use. On the other hand, the amount of data is another type of data deficiency problem. In this study, three-year monthly energy usage dataset was applied in the district-scale building energy modeling with LSTM, which could be one of the main limitations in this study; however, in the future, this study will involve more datasets from the campus or other district-scale building groups for

further validation of the proposed model.

Secondly, according to the building network, creating networks between buildings that are more like human' networks and applying building networks in city-scale studies (e.g. modeling building energy use with reference buildings) are increasing, interesting, and significant research topics. This study used the historical monthly electricity use dataset to calculate the correlation between buildings, which denotes the network. Since the building network consisted of inputs for multi-building energy prediction, it could impact the implementation of the algorithm if the energy use dataset is not available. Therefore, it might be better to illustrate building networks using buildings' physical information when no electricity data is available. Physical-information-based building networks can be better applied in an urban building block integrated energy simulation.

Thirdly, occupancy rate and occupant behavior information are quite important whether in individual or district-/city-level building energy prediction [67–69]. However, such information changes dynamically and daily, and introduces obvious challenges to obtaining the relevant data, especially for district-/city-level buildings. Some other issues, such as weather conditions, are also important factors that influence the urban building model. This problem will be a vital issue for future research seeking to create UBEMs in simulation as well as data-driven techniques; meanwhile, it is also necessary and significant to compare data-driven with simulation techniques to find the potential of fusing two techniques to compensate for their respective weaknesses.

Finally, this study integrated the BN and LSTM as the predictive model and compared it with ANN and SVR models. However, other effective deep learning techniques (e.g. transfer learning, convolutional Neural Networks) exist. Such models could also be potentially significant in future works for a wider comparison of data-driven UBEMs and validation of adaptability of the approach.

6. CONCLUSION

This study proposed an integrated building network and the long short-term memory model to predict district-level building energy use. The building network was created by the coefficient between individual buildings in one building group, and the long short-term memory model was performed in the TensorFlow tool. This study used the Southeast University in Nanjing, China as the case study, and five types of buildings groups with monthly electricity datasets from years 2015 to 2018 on the old and new campuses were applied for validation. Finally, mean absolute percentage error and root mean square error indices were used for model assessment. Via comparisons of different types of buildings, the results revealed that the proposed model can achieve very good prediction accuracies in each type of building when compared with two machine learning models (artificial neural network and support vector regression models). For the total energy use intensity prediction of buildings on the two campuses, the long short-term memory model can achieve a mean absolute percentage error of 6.66% and root mean square error of 0.36 kWh/m^2, compared to 12.05% and 0.63 kWh/m^2 for the artificial neural network model and 11.06% and 0.89 kWh/m^2 for the support vector regression model, respectively.

Therefore, the proposed model can enhance multi-building prediction accuracy on the district level while considering building connections to reduce the dataset and time-series characteristics of building energy datasets. In the campus area, the high accuracy of district-level building electricity prediction results can also provide good feedback to department of general affair regarding the awareness of energy usage. Meanwhile, this study can benefit the intelligent management of the campus-level micro-gird to support a green campus. In the future, on one hand, this study might involve more datasets and influencing factors in the deep learning model to test the adaptability. On the other hand, this study can inspire the integration of deep learning techniques in district- or city-level renewable energy analysis according to the demand at building side and provide significant insights into data-driven techniques

for urban building energy models to understand the building energy dynamics and support sustainable studies on the district and city levels.

ACKNOWLEDGEMENT

The work described in this study was sponsored by the projects of the National Natural Science Foundation of China (NSFC#51678127), the National Scientific and Technological Support during the 12th Five-Year Plan Period (No.: 2013BAJ10B13), and China Scholarship Council (CSC#201706095035), and Beijing Advanced Innovation Center for Future Urban Design (UDC# 016010100). Any opinions, findings, conclusions, or recommendations expressed in this study are those of the authors and do not necessarily reflect the views of the National Scientific and Technological Support committee and NSFC. This work was also supported by the Assistant Secretary for Energy Efficiency and Renewable Energy, the U.S. Department of Energy under Contract No. DE-AC02-05CH11231.

REFERENCES

[1] Pérez-Lombard L, Ortiz J, Pout C. A review on buildings energy consumption information. Energy Build 2008;40:394–8. doi:10.1016/j.enbuild.2007.03.007.

[2] Hong T. IEA EBC annexes advance technologies and strategies to reduce energy use and GHG emissions in buildings and communities. Energy Build 2018;158:147–9. doi:10.1016/J.ENBUILD.2017.10.028.

[3] Kneifel J, Webb D. Predicting energy performance of a net-zero energy building: A statistical approach. Appl Energy 2016;178:468–83. doi:10.1016/J.APENERGY.2016.06.013.

[4] Li W, Zhou Y, Cetin K, Eom J, Wang Y, Chen G, et al. Modeling urban building energy use: A review of modeling approaches and procedures. Energy 2017;141:2445–57. doi:10.1016/j.energy.2017.11.071.

[5] Hsu D. Comparison of integrated clustering methods for accurate and stable prediction of building energy consumption data. Appl Energy 2015;160:153–63. doi:10.1016/j.apenergy.2015.08.126.

[6] Jain RK, Smith KM, Culligan PJ, Taylor JE. Forecasting energy consumption of multi-family residential buildings using support vector regression: Investigating the impact of temporal and spatial monitoring granularity on performance accuracy. Appl Energy 2014;123:168–78. doi:10.1016/j.apenergy.2014.02.057.

[7] Han Y, Taylor JE, Pisello AL. Toward mitigating urban heat island effects: Investigating the thermal-energy impact of bio-inspired retro-reflective building envelopes in dense urban settings. Energy Build 2015;102:380–9. doi:10.1016/J.ENBUILD.2015.05.040.

[8] Schaefer A, Ghisi E. Method for obtaining reference buildings. Energy Build 2016;128:660–72. doi:10.1016/j.enbuild.2016.07.001.

[9] Chen Y, Hong T. Creating Building Datasets for CityBES 2017.

[10] Hong T, Chen Y, Piette MA, Luo X. Modeling City Building Stock for Large-Scale Energy Efficiency Improvements using CityBES Commercial Building Energy Saver: An Energy Retrofit Analysis Toolkit View project Zero-net-energy (ZNE) buildings View project. ACEEE Summer Study Build. Energy Effic., 2018.

[11] Perera ATD, Coccolo S, Scartezzini JL, Mauree D. Quantifying the impact of urban climate by extending the boundaries of urban energy system modeling. Appl Energy 2018;222:847–60. doi:10.1016/j.apenergy.2018.04.004.

[12] Fonseca JA, Nguyen TA, Schlueter A, Marechal F. City Energy Analyst (CEA): Integrated framework for analysis and optimization of building energy systems in neighborhoods and city districts. Energy Build 2016;113:202–26. doi:10.1016/j.enbuild.2015.11.055.

[13] Nageler P, Zahrer G, Heimrath R, Mach T, Mauthner F, Leusbrock I, et al. Novel validated method for GIS based automated dynamic urban building energy simulations. Energy 2017;139:142–54. doi:10.1016/j.energy.2017.07.151.

[14] Remmen P, Lauster M, Mans M, Fuchs M, Osterhage T, Müller D. TEASER: an open tool for urban energy modelling of building stocks. J Build Perform Simul 2018;11:84–98. doi:10.1080/19401493.2017.1283539.

[15] Hu Y, White M, Ding W. An Urban Form Experiment on Urban Heat Island Effect in High Density Area. Procedia Eng 2016;169:166–74. doi:10.1016/j.proeng.2016.10.020.

[16] Perini K, Chokhachian A, Dong S, Auer T. Modeling and simulating urban outdoor comfort: Coupling ENVI-Met and TRNSYS by grasshopper. Energy Build 2017;152:373–84. doi:10.1016/j.enbuild.2017.07.061.

[17] Mostapha Sadeghipour Roudsari, Michelle Pak, Smith A. Ladybug: a Parametric Environmental Plugin for Grasshopper To Help Designers Create an Environmentally-Conscious Design. 13th Conf Int Build Perform Simul Assoc 2013:3129–35.

[18] Ladybug Tools | Honeybee n.d. https://www.ladybug.tools/honeybee.html.

[19] Bajšanski I V., Milošević DD, Savić SM. Evaluation and improvement of outdoor thermal comfort in urban areas on extreme temperature days:

Applications of automatic algorithms. Build Environ 2015;94:632–43. doi:10.1016/j.buildenv.2015.10.019.

[20] Xu X, Wu Y, Wang W, Hong T, Xu N. Performance-driven optimization of urban open space configuration in the cold-winter and hot-summer region of China. Build Simul 2019:1–14. doi:10.1007/s12273-019-0510-z.

[21] Taleb H, Musleh MA. Applying urban parametric design optimisation processes to a hot climate: Case study of the UAE. Sustain Cities Soc 2015;14:236–53. doi:10.1016/j.scs.2014.09.001.

[22] Cerezo Davila C, Reinhart CF, Bemis JL. Modeling Boston: A workflow for the efficient generation and maintenance of urban building energy models from existing geospatial datasets. Energy 2016;117:237–50. doi:10.1016/j.energy.2016.10.057.

[23] Pisello AL, Castaldo VL, Taylor JE, Cotana F. Expanding Inter-Building Effect modeling to examine primary energy for lighting. Energy Build 2014;76:513–23. doi:10.1016/J.ENBUILD.2014.02.081.

[24] Han Y, Taylor JE, Pisello AL. Exploring mutual shading and mutual reflection inter-building effects on building energy performance. Appl Energy 2017;185:1556–64. doi:10.1016/J.APENERGY.2015.10.170.

[25] Han Y, Taylor JE. Simulating the Inter-Building Effect on energy consumption from embedding phase change materials in building envelopes. Sustain Cities Soc 2016;27:287–95. doi:10.1016/J.SCS.2016.03.001.

[26] Zhao F, Lee SH, Augenbroe G. Reconstructing building stock to replicate energy consumption data. Energy Build 2016;117:301–12. doi:10.1016/J.ENBUILD.2015.10.001.

[27] Felsmann C, Robbi S, Eckstädt E. Reduced Order Building Energy System Modeling in Large-Scale. 13Th Conf Int Build Perform Simul Assoc 2013:1216–23.

[28] Heidarinejad M, Mattise N, Dahlhausen M, Sharma K, Benne K, Macumber D, et al. Demonstration of reduced-order urban scale building energy models. Energy Build 2017;156:17–28. doi:10.1016/j.enbuild.2017.08.086.

[29] U.S. Department of Energy. Commercial Prototype Building Models. Build Energy Codes Progr 2016:4–7.

[30] Ballarini I, Corgnati SP, Corrado V. Use of reference buildings to assess the energy saving potentials of the residential building stock: The experience of TABULA project. Energy Policy 2014;68:273–84. doi:10.1016/j.enpol.2014.01.027.

[31] Filogamo L, Peri G, Rizzo G, Giaccone A. On the classification of large residential buildings stocks by sample typologies for energy planning purposes. Appl Energy 2014;135:825–35. doi:10.1016/j.apenergy.2014.04.002.

[32] Mastrucci A, Baume O, Stazi F, Leopold U. Estimating energy savings for the residential building stock of an entire city: A GIS-based statistical downscaling approach applied to Rotterdam. Energy Build 2014;75:358–67. doi:10.1016/j.enbuild.2014.02.032.

[33] Caputo P, Costa G, Ferrari S. A supporting method for defining energy strategies in the building sector at urban scale. Energy Policy 2013;55:261–70. doi:10.1016/j.enpol.2012.12.006.

[34] Xu X, Wang W, Hong T, Chen J. Incorporating machine learning with building network analysis to predict multi-building energy use. Energy Build 2019;186:80–97. doi:10.1016/J.ENBUILD.2019.01.002.

[35] Deb C, Lee SE. Determining key variables influencing energy consumption in office buildings through cluster analysis of pre- and post-retrofit building data. Energy Build 2018;159:228–45.

[36] Arambula Lara R, Pernigotto G, Cappelletti F, Gasparella A. Energy audit of schools by means of cluster analysis. Energy Build 2015;95:160–71. doi:10.1016/J.ENBUILD.2015.03.036.

[37] Tardioli G, Kerrigan R, Oates M, O'Donnell J, Finn DP. Identification of representative buildings and building groups in urban datasets using a novel pre-processing, classification, clustering and predictive modelling approach. Build Environ 2018;140:90–106. doi:10.1016/J.BUILDENV.2018.05.035.

[38] Yang Z, Roth J, Jain RK. DUE-B: Data-driven urban energy benchmarking of buildings using recursive partitioning and stochastic frontier analysis. Energy Build 2018;163:58–69. doi:10.1016/J.ENBUILD.2017.12.040.

[39] Gaitani N, Lehmann C, Santamouris M, Mihalakakou G, Patargias P. Using principal component and cluster analysis in the heating evaluation of the school building sector. Appl Energy 2010;87:2079–86. doi:10.1016/J.APENERGY.2009.12.007.

[40] Zhao HX, Magoulès F. A review on the prediction of building energy consumption. Renew Sustain Energy Rev 2012;16:3586–92. doi:10.1016/j.rser.2012.02.049.

[41] Kadir Amasyali, Nora M. El-Gohary. A review of data-driven building energy consumption prediction studies. Renew Sustain Energy Rev 2018;81:1192–205. doi:10.1016/J.RSER.2017.04.095.

[42] Guo Y, Wang J, Chen H, Li G, Liu J, Xu C, et al. Machine learning-based thermal response time ahead energy demand prediction for building heating systems. Appl Energy 2018;221:16–27. doi:10.1016/J.APENERGY.2018.03.125.

[43] Wei Y, Xia L, Pan S, Wu J, Zhang X, Han M, et al. Prediction of occupancy level and energy consumption in office building using blind system

identification and neural networks. Appl Energy 2019;240:276–94. doi:10.1016/J.APENERGY.2019.02.056.

[44] Fan C, Wang J, Gang W, Li S. Assessment of deep recurrent neural network-based strategies for short-term building energy predictions. Appl Energy 2019;236:700–10. doi:10.1016/j.apenergy.2018.12.004.

[45] Wang Z, Hong T, Piette MA. Data fusion in predicting internal heat gains for office buildings through a deep learning approach. Appl Energy 2019;240:386–98. doi:10.1016/J.APENERGY.2019.02.066.

[46] Masaki M, Zhang, Lijun, Xia X. A hierarchical predictive control strategy for renewable grid integrated hybrid energy storage systems. Appl Energy 2018;submitted:393–402.

[47] González-Aparicio I, Zucker A. Impact of wind power uncertainty forecasting on the market integration of wind energy in Spain. Appl Energy 2015;159:334–49. doi:10.1016/j.apenergy.2015.08.104.

[48] Heiple S, Sailor DJ. Using building energy simulation and geospatial modeling techniques to determine high resolution building sector energy consumption profiles. Energy Build 2008;40:1426–36. doi:10.1016/J.ENBUILD.2008.01.005.

[49] Chen Y, Hong T, Piette MA. Automatic generation and simulation of urban building energy models based on city datasets for city-scale building retrofit analysis. Appl Energy 2017;205:323–35.

[50] Li C, Hong T, Yan D. An insight into actual energy use and its drivers in high-performance buildings. Appl Energy 2014;131:394–410. doi:10.1016/j.apenergy.2014.06.032.

[51] Kontokosta CE, Tull C. A data-driven predictive model of city-scale energy use in buildings. Appl Energy 2017;197:303–17. doi:10.1016/j.apenergy.2017.04.005.

[52] Deng H, Fannon D, Eckelman MJ. Predictive modeling for US commercial building energy use: A comparison of existing statistical and machine learning algorithms using CBECS microdata. Energy Build 2018;163:34–43. doi:10.1016/j.enbuild.2017.12.031.

[53] Robinson C, Dilkina B, Hubbs J, Zhang W, Guhathakurta S, Brown MA, et al. Machine learning approaches for estimating commercial building energy consumption. Appl Energy 2017;208:889–904. doi:10.1016/j.apenergy.2017.09.060.

[54] Fonseca JA, Schlueter A. Integrated model for characterization of spatiotemporal building energy consumption patterns in neighborhoods and city districts. Appl Energy 2015;142:247–65. doi:10.1016/j.apenergy.2014.12.068.

[55] Kalogirou S, Neocleous C, Schizas C. Building Heating Load Estimation Using Artificial Neural Networks. Proc 17th Int Conf Parallel Archit Compil Tech 1997:1–8.

[56] Hawkins D, Hong SM, Raslan R, Mumovic D, Hanna S. Determinants of energy use in UK higher education buildings using statistical and artificial neural network methods. Int J Sustain Built Environ 2012;1:50–63. doi:10.1016/j.ijsbe.2012.05.002.

[57] Kavgic M, Summerfield A, Mumovic D, Stevanovic Z. Application of a Monte Carlo model to predict space heating energy use of Belgrade's housing stock. J Build Perform Simul 2015;8:375–90. doi:10.1080/19401493.2014.961031.

[58] Kavgic M, Mumovic D, Summerfield A, Stevanovic Z, Ecim-Djuric O. Uncertainty and modeling energy consumption: Sensitivity analysis for a city-scale domestic energy model. Energy Build 2013;60:1–11. doi:10.1016/J.ENBUILD.2013.01.005.

[59] TensorFlow n.d. https://www.tensorflow.org/.

[60] Abadi M, Agarwal A, Barham P, Brevdo E, Chen Z, Citro C, et al. TensorFlow: Large-Scale Machine Learning on Heterogeneous Distributed Systems 2016.

[61] Hochreiter S, Schmidhuber J. Long Short-Term Memory. Neural Comput 1997;9:1735–80. doi:10.1162/neco.1997.9.8.1735.

[62] Graves A, Liwicki M, Fernandez S, Bertolami R, Bunke H, Schmidhuber J. A Novel Connectionist System for Unconstrained Handwriting Recognition. IEEE Trans Pattern Anal Mach Intell 2009;31:855–68. doi:10.1109/TPAMI.2008.137.

[63] Sak H, Senior A, Beaufays F. Long Short-Term Memory Based Recurrent Neural Network Architectures for Large Vocabulary Speech Recognition 2014.

[64] Li X, Wu X. Constructing Long Short-Term Memory based Deep Recurrent Neural Networks for Large Vocabulary Speech Recognition 2014.

[65] Wang W, Chen J, Hong T, Zhu N. Occupancy prediction through Markov based feedback recurrent neural network (M-FRNN) algorithm with WiFi probe technology. Build Environ 2018;138:160–70. doi:10.1016/J.BUILDENV.2018.04.034.

[66] ENERGY.GOV. Buildings and the Grid 101: Why Does it Matter for Energy Efficiency 2017. https://energy.gov/eere/buildings/articles/buildings-and-grid-101-why-does-it-matter-energy-efficiency.

[67] Hong T, Yan D, D 'oca S, Chen C-F. Ten questions concerning occupant behavior in buildings: The big picture. Build Environ 2017;114:518–30. doi:10.1016/j.buildenv.2016.12.006.

[68] Wang W, Hong T, Li N, Wang RQ, Chen J. Linking energy-cyber-physical systems with occupancy prediction and interpretation through WiFi probe-based ensemble classification. Appl Energy 2019;236:55–69. doi:10.1016/J.APENERGY.2018.11.079.

[69] Wang W, Chen J, Huang G, Lu Y. Energy efficient HVAC control for an IPS-enabled large space in commercial buildings through dynamic spatial occupancy distribution. Appl Energy 2017. doi:10.1016/J.APENERGY.2017.06.060.